Lab on a Chip

Accepted Manuscript

ROYAL SOCIETY OF CHEMISTRY

www.rsc.org/loc

Cite this: DOI: 10.1039/c0xx00000x

www.rsc.org/xxxxxx

ARTICLE TYPE

Moving droplets between closed and open microfluidic systems

Weiqiang Wang,*[a] and Thomas B. Jones[b]

Received (in XXX, XXX) Xth XXXXXXXXX 20XX, Accepted Xth XXXXXXXXX 20XX
DOI: 10.1039/bxxxxxx

In electric-field-mediated droplet microfluidics, there are two distinct architectures - closed systems using parallel-plate electrodes and open systems using coplanar electrodes fabricated on an open substrate. An architecture combining both closed and open systems on a chip would facilitate many of the chemical and biological processes now envisioned for the laboratory on a chip. To accomplish such an integration requires a means to move droplets back and forth between the two. This paper presents an investigation of the requirements for such manipulation of both water and oil droplets. The required wetting conditions for a droplet to cross the open/closed boundary is revealed by a force balance analysis and predictions of this model are compared to experimental results. Water droplets can be moved between closed and open systems by electrowetting actuation; droplet detachment from the upper plate is facilitated by the use of beveled edge. The force model predicts that driving an oil droplet from a closed to an open structure requires an oleophobic surface. This prediction has been tested and confirmed using <100> silicon wafers made oleophobic by re-entrant microstructures etched into the surface.

Introduction

Droplet-based microfluidics is based on individuated liquid droplets – sometimes arrays of them – which are manipulated, transported, mixed, and divided to achieve useful ends in lab-on-a-chip applications. Droplet-based schemes are useful because they reduce consumption of costly reagents, shorten analysis times, and provide inherent flexibility. The essential droplet manipulations can be achieved with patterned, individually addressable electrodes, using electrowetting[1-7] (EW) and/or dielectrophoresis[6-12] (DEP). To enlist these electrical forces, liquid droplets are sandwiched between two parallel plates or placed on an open substrate patterned with co-planar electrodes. In this paper, we refer to these two architectures as closed and open microfluidic systems, respectively.

The closed systems consist of two parallel substrates with the droplet sandwiched between them. See Fig. 1. Usually, an array of individually addressable electrodes is patterned on the bottom substrate, and the top substrate, with a conductive and transparent coating, serves as a continuous ground electrode. The bottom substrate is over-coated with a dielectric layer, and then both the top and bottom surfaces are covered with a thin hydrophobic film such as Teflon to decrease surface wettability. Fig. 2 shows a typical open structure, consisting of an insulating substrate upon which coplanar electrodes are patterned. Again, the electrodes are coated with dielectric and a hydrophobic layers and the sessile droplet rests on top. Several open electrode designs have been reported, the principal distinction among them being the configuration of the ground electrode[13-17]. Abdelgawad et al.[18] investigated the performance of six different open configurations, used the results to optimize device design, and claimed the strongest actuation force for the configuration with a grounded metal wire. A problem with this scheme, however, is that the liquid can adhere to the wire and become difficult to separate, especially in the case of oils.

Fig. 2 illustrates top and side views of the coplanar electrode structure utilized in our study. The substrate is patterned with two arrays of electrodes – those on one side being grounded and those on the other side individually addressable.

Closed and open microfluidic systems each have distinct advantages. Closed systems can achieve the four basic fluidic operations: dispensing, transport, splitting, and merging of droplets. They also provide reliable, reproducible droplet volume control. While open structures cannot easily split droplets, they offer direct access for other liquid handling and manipulation tools and/or surface analytical equipment[17,18]. Mixing and evaporation (for concentration of species) are also easier in the open structures. A third advantage for open structures is that the ball-like droplet could focus the fluorescence and thus enhance the detection sensitivity[19]. Because electric actuation is such a versatile fluid handling tool, both closed and open microfluidic systems have been considered for large numbers of lab-on-a-chip applications. These approaches are detailed in several review papers[1,5,20]. For closed systems, although many applications can be realized by integration with in-line (droplets are analyzed

[a] *Department of Mechanical Engineering, Nanjing University of Science and Technology, Nanjing, Jiangsu 210094 China. Fax: +86-25-84315831; Tel: +86-13951676028; Email: wangweiqiang@njust.edu.cn*
[b] *Department of Electrical and Computer Engineering, University of Rochester, Rochester, NY 14627 USA. Tel: (585) 275-5233; Email: Jones@ece.rochester.edu*
†Electronic Supplementary Information (ESI) available: Movies.

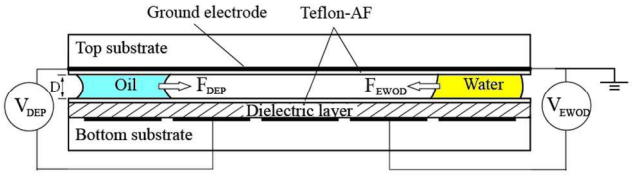

Fig. 1 Cross-section of a parallel-plate (closed) device to manipulate oil and water droplets by DEP and EWOD, respectively.

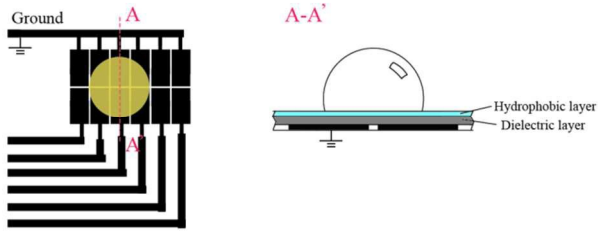

Fig. 2 Schematic of co-planar electrode configuration. Ground potential is connected to an array of electrodes parallel to actuation electrodes. Left: top view; Right: side view.

within a device) analysis methods[5], certain complex applications require the droplets to be removed from the chip for off-line processing, such as purification[21], bio-culturing[22], MS evaluation[23,24], or other protocols[25]. For open systems, one critical off-line process is sample loading, where droplets are loaded onto the chip using micro-pipettes[14-17,26]. This sort of operation is cumbersome and affects reproducibility. One way to automate these off-line processes is to integrate open and closed systems. Then, droplet might be dispensed within the closed structure from a large reservoir after which desired droplet manipulation and analytical operations can be done in either closed or open structures, depending on process requirements, and finally the droplets can be transferred away for other operations or harvested off the open structure.

Furthermore, integrated closed/open systems can facilitate interconnection of different microfluidic devices. Indeed, the interconnection of droplet-based microfluidic systems with microflow systems would represent a substantial advance for lab-on-a-chip technology. Presently only a few examples have been reported to convert a droplet or a digital microflow into a continuous flow[27-29]; and the converse operation, that is, extracting micro-drops from a continuous flow, is still largely underdeveloped. It should be obvious that integration of closed and open electrically actuated systems is critical for the second scheme to extract droplets and insert them into a digital microfluidic device. Samples of fluid exiting a micro-channel can be collected into droplets on an open surface (for example, by sweep deposition[30]), and droplets thus formed can be transported on the open structure or delivered into closed structure for further processes. Such a scheme capable of extracting droplets from a continuous flow would benefit several applications as anticipated by Berthier et al.[31]. On the other hand, when the droplet is moved from closed structure to an open surface, it becomes convenient to transfer the droplet into a second fluid bath to form suspending double emulsion droplet, this scheme is useful for precisely controlled laser target fabrication[32].

The critical operation for integrating closed and open system as defined in this paper is to move droplets across the boundary from one structure to the other. Berthier et al. considered this problem by analyzing the pressure evolution within a droplet during its transport across the boundary between the two sections[33]. By calculating droplet pressure in each section, he identified domains where (i) spontaneous motion from open to closed regions is not allowed when the gap spacing is too small and (ii) motion in the opposite direction is impossible when the gap is too large. He reported droplet motion experiments at different gap spacing to test the predictions of his analytical model. More recently, Wang et al. demonstrated back and forth motions of a water droplet between open and closed regions using non-parallel electrodes[34]. His analysis of drop motion mechanisms is also based on pressure. However, because the pressure calculation requires contact angle information to derive interfacial radii of curvature, it is difficult to evaluate the pressure difference of dielectric droplets (or aqueous droplets subjected to high frequency electric field), as these droplets exhibit virtually no change in contact angle under electric actuation[6,35]. As an alternative, the method of force balance analysis is a direct way to quantitatively evaluate droplet motion between closed and open structures. In this case, electric actuation forces can be calculated conveniently using the electromechanical model[35-37]. Because the model requires no information about contact angle or liquid profile[35], it is well-suited for force calculations on both aqueous and non-aqueous (dielectric) liquid droplets.

The present work introduces predictive models for droplet motion between closed and open microfluidic systems and then reports experiments to verify the model. We first employ an argument based on Gibbs free energy to predict the preferred directions for spontaneous droplet motion across the boundary between the two structures. Next follows an evaluation of the actuation voltage required for successful motion using force balance analysis. Based on these analyses, we propose and test improved device structures to facilitate droplet motion, including

Table 1 Properties and profile parameters for 100 nL droplets in closed and open structures. Note the large difference in the contact diameters (a) of sessile water and oil droplets. w is the droplet contact diameter in closed section when gap spacing is 100 μm.

	Surface tension (mN/m)	Dielectric constant	Contact angle (°)	Drop volume (nL)	Gap spacing of closed section (μm)	w (mm)	a (mm)
water	74	78	115	100	100	1.1	0.56
silicone oil (20 cst)	20.6	2.68	53	100	100	1.1	0.98
mineral oil	28.1	2.2	74	100	100	1.1	0.83

a beveled edge to assist in droplet detachment from upper substrate and the use of oleophobic surface treatment to eject dielectric (oil) droplets. Droplet attachment to a solid surface is a common phenomenon, and it can interfere with droplet motion from a closed to an open structure, especially when the liquid droplet is in air medium. The beveled edge structure effectively solves this problem by minimizing the liquid-solid contact area and reduces the droplet detachment voltages by up to a factor of three. Force analysis also explains the difficulty of moving oil droplets across the open/closed boundary and suggests the efficacy of requirement for oleophobic surfaces. Finally, experiments are performed to demonstrate the predicted droplet motion for both aqueous and oil droplets between closed and open sections.

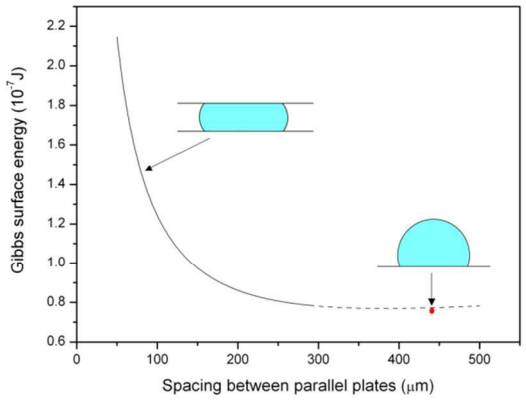

(a)

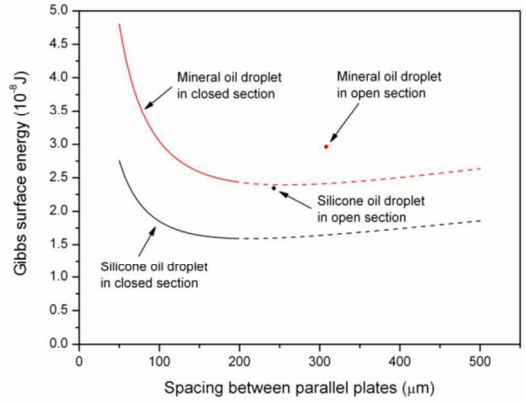

(b)

Fig. 3 (a) Calculated Gibbs free energy for 100 nL water droplet in parallel-plate structure (line) and single-plate structure (red dot). (b) Gibbs free energy of a 100 nL oil droplet in closed structure (line) and open structure (dot). Red: mineral oil droplet; Black: Silicone oil (20 cst) droplet. When the gap height is large, model is less accurate due to droplet distortion as indicated by dashed portion of curve.

Gibbs energy model

Calculation and comparison of the Gibbs free energy values for liquid droplets facilitates identification of the preferred hydrostatic configurations for droplet within closed/open systems. The Gibbs surface energy is a sum of the products of interfacial tensions and their corresponding surface areas. The calculation for a droplet trapped between two parallel surfaces is based on a previously reported model[7]. For a sessile droplet resting on an open substrate, knowledge about droplet shape is needed. Here, we assume the droplet can be approximated as a spherical cap[31]. For simplification, the calculations ignore any energy barrier at the closed/open boundary. All calculations represented in Figs. 3a and b have been performed for a 100 nL droplet and employ the appropriate contact angle and interfacial tension values for water or oil taken from Table 1.

Fig. 3a plots Gibbs surface energy for a water droplet as a function of D, the spacing between the parallel plates. The surface energy falls rapidly as D increases. For comparison, the Gibbs surface energy is also plotted for a sessile droplet of the same volume resting on an open substrate. When the gap spacing is ≤ 100 μm, the value for the sessile droplet is much lower than that for the droplet in a closed section. Thus, for gaps of the order of 100 μm or less, it is energetically favorable to move a 100 nL water droplet from a closed to an open section. On the other hand, energy is required to move a droplet from an open substrate into a closed structure.

The Gibbs surface energies for 100 nL droplets of silicone and mineral oils in both closed and open sections are plotted in Fig. 3b. Just as for a water droplet, the total surface energy of oil droplets decreases with the gap spacing. Unlike water droplets, however, the Gibbs surface energy of sessile oil droplets in an open section is higher than that in the closed structure. Thus, an oil droplet lodged between parallel plates is the more energetically favored state. The model thus predicts that it is easier to move an oil droplet from an open section to a closed section than to the reverse.

Force balance analysis

The force balance analysis is done by comparing the electric actuation force with the resisting forces. Because the electric actuation force is a function of external applied voltage, it is convenient to estimate voltage requirements for droplet motion in either direction between closed and open structures from this force analyses.

Water droplet motion between open and closed structures

For the case of a water droplet moving from a closed structure to an open substrate, the interfacial forces exerted on the droplet at the boundary are illustrated in Fig. 4b. Because there is no displacement of the upper portion of the droplet that contacts the edge of the ITO plate, the influence of F_4 can be neglected. Then, the total surface tension force acting on the drop is:

$$F_{total} = F_3|\cos\theta_V| + (F_1 - F_5)|\cos\theta| + F_2|\cos\theta| \quad (1)$$

where $F_1 = F_2 = \gamma w$, $F_3 = \gamma a$, $F_5 = \gamma(w\text{-}a)$, w and a are contact lengths of the droplet in closed and open regions, respectively, and θ_V and θ are the droplet contact angle with and without applied voltage, also respectively. Note that the EWOD contribution is accounted for in Eq. (1) as a voltage-dependent change in the contact angle θ_V.

Here, when θ_V is reduced below 90°, the lateral components of F_3, F_2, and (F_1-F_5) in Eq. (1) all aid in moving the droplet toward the open side, so it is understandable that the droplet easily exits

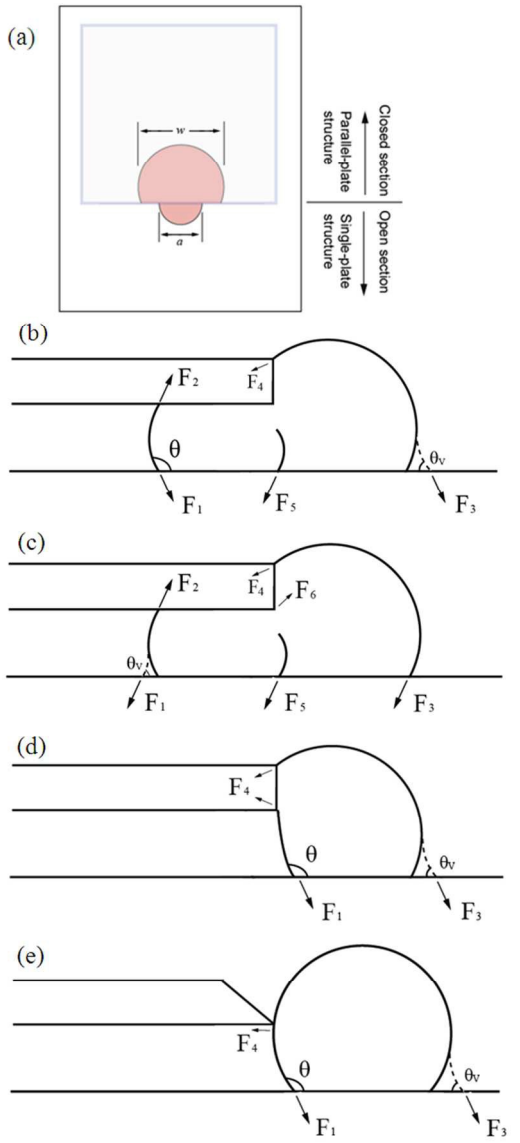

Fig. 4 Interfacial force balance for a water droplet at the closed/open boundary. (a) Top view of a water droplet at the closed/open boundary. (b) Interfacial forces exerted on a water droplet at the closed/open boundary when it is being moved toward the open region. (c) Interfacial forces exerted on a water droplet at the closed/open boundary when it is being moved toward the closed region. (d) and (e) Interfacial forces exerted on a water droplet at open region but stuck to the upper ITO plate: (d) a normal ITO plate; (e) ITO plate with beveled edge.

the closed section. In fact, the water droplet is expelled even without external applied voltage, in which case the total lateral force is just $F_2|\cos\theta|$. One might anticipate a metastable state at the closed/open boundary in the case where $F_2|\cos\theta|$ is too small to overcome contact angle hysteresis, but the electric force can easily overcome any metastable state that might exist.

Figure 4c depicts the force components for the case where a water droplet is being moved back into the closed region from the open substrate. Here, the total force becomes:

$$F_{total} = F_1|\cos\theta_v| + (F_3 + F_5)|\cos\theta| - F_2|\cos\theta| - F_6|\cos\beta| \quad (2)$$

F_4 is again ignored because its effect is just to pull the droplet up and down, any horizontal component being compensated by the ITO plate. F_6 is the resisting force from the top ITO plate due to droplet deformation. We estimate that the lateral portion of F_6 is equal to $F_5|\cos\theta|$, then

$$F_{total} = F_1|\cos\theta_v| + F_3|\cos\theta| - F_2|\cos\theta|$$
$$= \gamma w|\cos\theta_v| + \gamma a|\cos\theta| - \gamma w|\cos\theta| \quad (3)$$

According to Eq. (3), $F_{total} > 0$ leads to the requirement that $\cos\theta_V > (w\text{-}a)|\cos\theta|/w$ for the contact angle. Thus a threshold value of θ_V can be defined as $\arccos[(w\text{-}a)|\cos\theta|/w]$, EW actuation must effectively reduce the contact angle below this threshold value to move droplet into the closed structure. The contact angle threshold is calculated as a function of droplet volume at different gap spacings, as shown in Figure 5a. This result shows that the contact angle threshold decreases with reduced gap spacing and increased droplet volume. Because the minimum contact angle achieved by EW actuation is ~78° due to the saturation limit, droplet motion into closed structure would be impossible when the gap spacing is too small or the liquid droplet is too large. This result is consistent with Berthier's analysis[33].

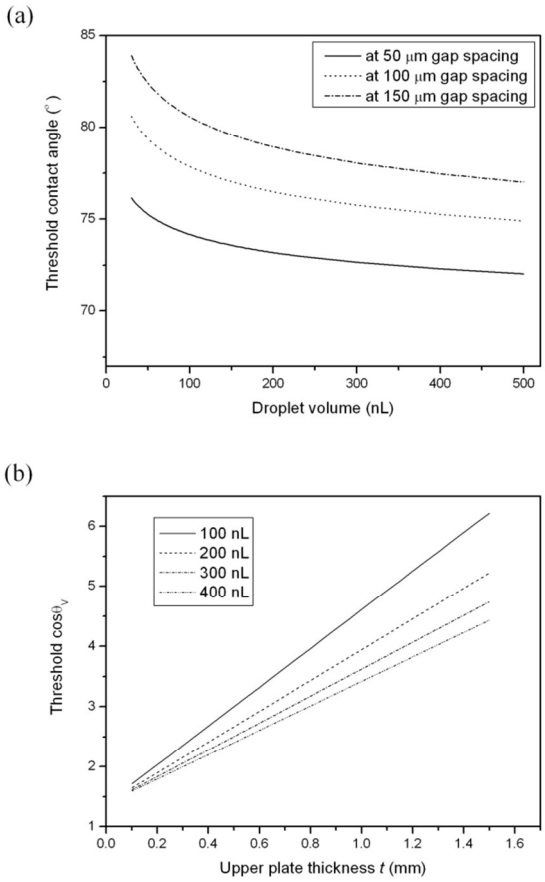

Fig. 5 (a) Threshold contact angle values for successful droplet motion from open to closed structure. (b) Threshold $\cos\theta_V$ for successful droplet detachment. Note that all the required $\cos\theta_V$ values are greater than 1.

Detaching a water droplet from upper (ITO) plate

When the droplet emerges from the closed section, it tends to stick to the Teflon-coated ITO glass due to the low interfacial tension between water and Teflon surface as depicted in Figure 4d. Now the resisting force is the lateral component of F_4, so for successful droplet detachment, the electrical actuation force must

overcome F_4:

$$F_{total} = F_E - F_4\sin\theta$$
$$= (F_1|\cos\theta| + F_3|\cos\theta_v|) - F_4\sin\theta$$
$$= \gamma a(|\cos\theta| + |\cos\theta_v|) - \gamma(2a + 2t)\sin\theta \quad (4)$$

where t is the thickness of ITO plate.

To achieve $F_{total} > 0$, $\cos\theta_V$ must be greater than the threshold value of $[\cos\theta+2(a+t)\sin\theta/a]$. Figure 5b shows the linear relationship between threshold $\cos\theta_V$ and t. It is apparent that this threshold increases directly with increased t or reduced droplet volume. Thus one may expect easier droplet detachment with a thin upper substrate or a large drop. However, an unusual result in Figure 5b is that all the threshold $\cos\theta_V > 1$. This non-physical result means that $F_{total} > 0$ is unachievable. This conclusion reveals a limit of the contact angle interpretation of electrowetting, namely that the maximum EW force from the contact angle model is $\gamma a(|\cos\theta|+1)$. This term can never be large enough to detach the water droplet. Instead, we can invoke the electromechanical model to calculate the net EW force, which does not consider changes to the contact angle and thus avoids the apparent paradox[35,37]. Refer to the calculation model in ESI. By substituting the droplet and device parameters into Eq. (S8) with the electric force F_E expressed in terms of applied voltage, we obtain the condition $V > 244$V for $F_{total} > 0$. This voltage value is consistent with the experiment described in next section.

Eq. (4) teaches that the detachment voltage will be reduced for a larger droplet (increasing a) or a thinner upper plate (reducing t). Droplet volume is usually fixed by other considerations, but the edge of the ITO glass plate can be beveled to reduce the water/Teflon contact area ($t \rightarrow 0$) as shown in Figure 4e. With this method, F_4 is reduced to γa and the required voltage is 105 V.

Oil droplet motion between open and closed structures

Oil droplets have low surface tension and exhibit low contact angle on most solid surfaces. This is why oils always seem to find their way into cracks or small gaps. We can overcome this tendency to move oil droplets from a closed channel to an open substrate using the DEP force. Because most oils are insulative, the contact angle is virtually unaffected by an applied electric field[6]. Fig. 6a depicts the force contributions for an oil droplet at the boundary between closed and open regions in a microfluidic device. The total force acting on the droplet is:

$$F_{total} = F_{DEP} - F_2\cos\theta - F_4\sin\theta + (F_3\cos\theta + F_5\cos\theta - F_1\cos\theta)$$
$$\approx F_{DEP} - F_2\cos\theta - F_4\sin\theta \quad (5)$$

With no applied voltage, the oil droplet is naturally drawn into the closed region. The more challenging problem, then, is to move an oil droplet from the closed into the open region. The DEP force that appears in Eq. (5) can be calculated using Eq. (S8). Here, $F_2 = \gamma w$ and $F_4 = \gamma a$, w and a are the contact lengths of the droplet in the closed and open sections, respectively. Using the parameters from Table 1 and Table A1, the predicted voltages to achieve the threshold $F_{total} = 0$ are 1292 V and 1555 V for silicone oil and mineral oil, respectively. The electric field values for these voltages considerably exceed the dielectric breakdown strength of the device dielectric layers. Thus, it would seem to be impossible to expel an oil droplet from between two plates by direct DEP actuation.

One proposed solution is to use non-parallel plates as shown in Figure 6b. If the upper plate is slightly tilted, it might be possible to drive the oil droplet from a narrow region to a wide region, and

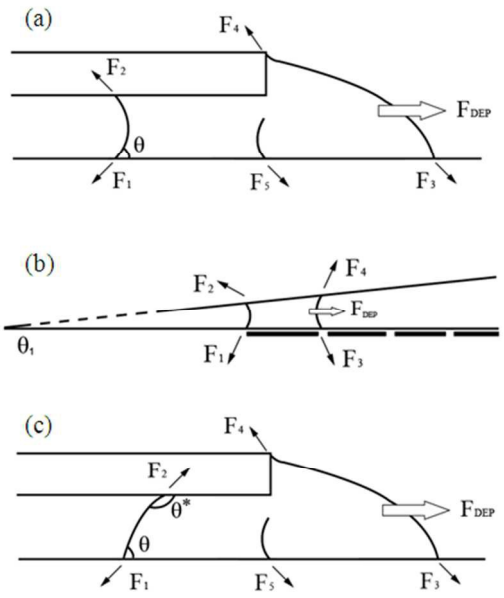

Fig. 6 (a) Interfacial forces for an oil droplet at the closed/open boundary with oleophilic surfaces. (b) Non-parallel two-plate structure to drive the oil droplet from narrow region to wide region by DEP. (c) Force balance analysis of an oil droplet at the closed/open boundary with oleophobic top surface.

eventually to deliver the oil droplet to an open section. The total force acting on the oil droplet is:

$$F_{total} = F_{DEP} - [F_1\cos\theta + F_2\cos(\theta - \theta_1) - F_3\cos\theta - F_4\cos(\theta + \theta_1)]$$
$$= F_{DEP} - 2\gamma w\sin\theta\sin\theta_1 \quad (6)$$

where θ_1 is the tilt angle of the upper plate. Because the upper plate is only slightly tilted, the parallel-plate approximation of Eq. (S8) can still be used to calculate the DEP force. From Eq. (6), $F_{total} > 0$ gives $\sin\theta_1 < F_{DEP}/2\gamma w\sin\theta = 0.15$, so the tilt angle θ_1 must be small to ensure successful actuation of oil droplets.

Although actuation of an oil droplet can be achieved in the non-parallel two-plate scheme, there remains the problem that the oil droplet tends to break up as it is ejected from the closed section. One can gain an understanding of this phenomenon by considering the process of separating two plates slowly. Refer to Fig. 7a showing oil droplet between parallel plates with contact angle $\theta < 90°$. The vertical component of the surface tension forces at the upper (or lower) edge and the middle of drop are respectively:

$$F_{edge} = \gamma 2\pi R\sin\theta \quad (7)$$

and

$$F_m = \gamma 2\pi r \quad (8)$$

As the plates separate, both R and r decrease. At some point F_{edge} will exceed F_m because r can approach 0. Then, the droplet breaks into two droplets, one each on the top and bottom substrates. We find that oil droplets exhibit this behavior in the non-parallel structure of Fig. 6b, breaking up on arrival at the open section. Kang et al. has reported this droplet break-up mechanism[38].

In contrast, this breakup does not occur for water droplets on Teflon-coated substrates because the contact angle is greater than 90°, as depicted in Fig. 7b. Because $R < r$, the vertical component of the surface tension force at the upper (or lower) edge, F_{edge}, is

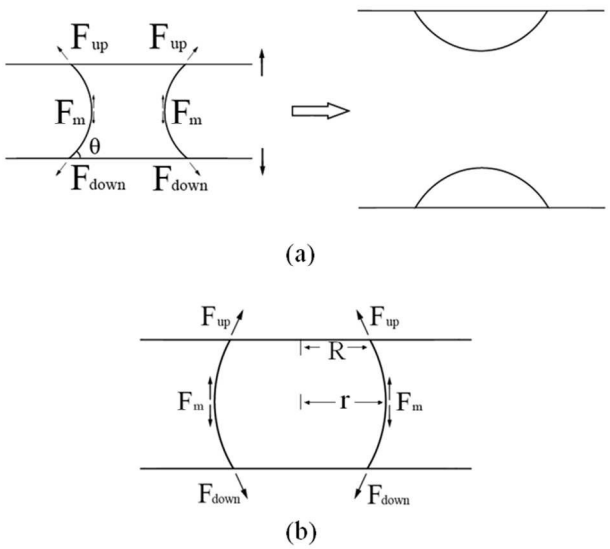

Fig. 7 (a) Break-up of bridging oil droplet in parallel-plate structure when two plates separate. (b) The profile of a water droplet sandwiched between parallel plates.

always smaller than F_m. Thus, the droplet can detach from one surface without splitting as reported by Wang et al[34].

Summary

In summary, the liquid/solid contact angle plays an important role in keeping a droplet from splitting during its closed-to-open movement. When the contact angle is < 90°, the droplet has a "slim waist" profile in the parallel-plate structure, which can rupture easily before entering the open section. The solution to this problem is to employ an *oleophobic* surface on one of the parallel-plate surfaces. In such a structure, as depicted in Fig. 6c, the total force acting on the oil drop becomes

$$F_{total} = F_{DEP} + F_2|\cos\theta^*| - F_4\sin\theta \quad (9)$$

Here, the vertical edge of the upper plate is still assumed oleophilic. $\theta^* > 90°$ is the oil contact angle against the top surface. F_2 and F_4 largely offset each other so the oil droplet can be transferred between open and closed regions by DEP actuation without splitting.

Experiment

To test the modeling predictions, we fabricated experimental structures from glass substrates divided into two parts and then patterned electrodes on one side for the closed system and the electrodes on the other side for the open system. The electrodes on the substrate are patterned by wet etching of a 100 nm layer of evaporatively deposited Al[7]. A 0.5 μm thick layer of spin-on-glass (Futurrex IC1-200) covering the electrodes serves as the dielectric layer, which is then coated with ~1 μm of amorphous fluoropolymer (Dupont Teflon-AF). The grounded, upper conductive plate of transparent ITO-coated glass, also Teflon-coated to make it hydrophobic for experiments with water droplets, is positioned above the closed section with spacers. See Fig. 8a. The bottom substrate is mounted horizontally and spring-loaded (Pogo) pins make electrical contact with pads on the surface. Voltages are applied to individually addressed electrodes using miniature electromechanical relays controlled by a programmable LabVIEW™-based system. A custom-made video system equipped with imaging lenses (Edmund EVA8X) and a CCD camera (JAI CV-S3200) records droplet actuation experiments at 30 fps.

Water droplet movement between closed and open regions

Roux et al. demonstrated that water droplets in an oil medium could be moved back and forth readily between closed and open microfluidic structures using electrical forces[39]. Here we test such manipulations in air. Fig. 8 contains a sequence of video frames demonstrating a water droplet moving from the closed section on the right to the open substrate on the left. The closed section has a gap spacing of 90 μm. When voltage is appropriately applied to the patterned electrodes in the closed section, a droplet injected into the closed section moves toward the boundary by EWOD actuation. When the droplet reaches the edge, it is ejected rapidly, but still tends to cling to the upper plate. See Fig. 8d. The droplet crosses the boundary, captured in Figs. 8b, c, and d, within 0.24 second. To detach the droplet from the upper ITO plate, a voltage ranging from 100 to 300 V_{rms} is briefly applied to the patterned electrodes of the open section. Detachment is successful at 300 V_{rms}, in reasonable agreement with the model's prediction of >244 V_{rms}. When the upper ITO plate is polished to form beveled edge, the detachment voltage is reduced to ~90 V_{rms}, in reasonable agreement with the prediction of 105 V_{rms}. Refer to Fig. 9.

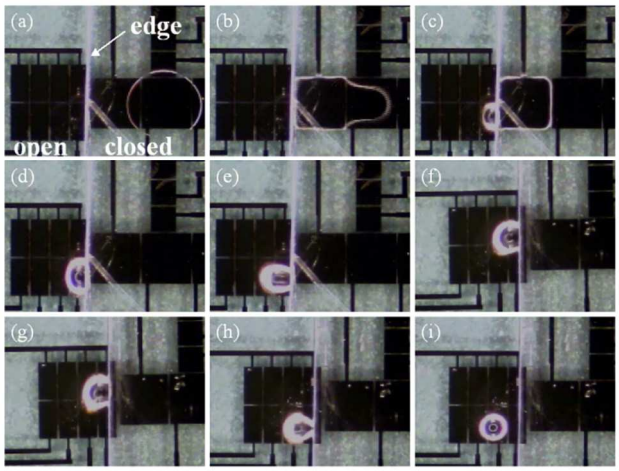

Fig. 8 Moving a water drop from closed to open section. (a) The water droplet is initially placed in closed section. (b) The droplet is moved towards closed/ open boundary by EWOD actuation using 100 V_{rms} 100 Hz AC. (c) The droplet enters open section as soon as it arrives at the boundary. (d) The droplet completely acrosses the boundary. (e)-(h) Different voltages are applied to remove the droplet from ITO plate: (e) 100 V_{rms} (f) 120 V_{rms} (g) 180 V_{rms} (h) 300 V_{rms}.(i) The droplet is successfully removed after applying 300 V_{rms} voltage. The spacing between two plates for the closed section is 90 μm, and the thickness of upper plate is 1.12 mm. DI water droplet volume is 380 nL. All the voltages are AC at 100 Hz. Video 01 can be seen in the ESI.

Cite this: DOI: 10.1039/c0xx00000x

www.rsc.org/xxxxxx

ARTICLE TYPE

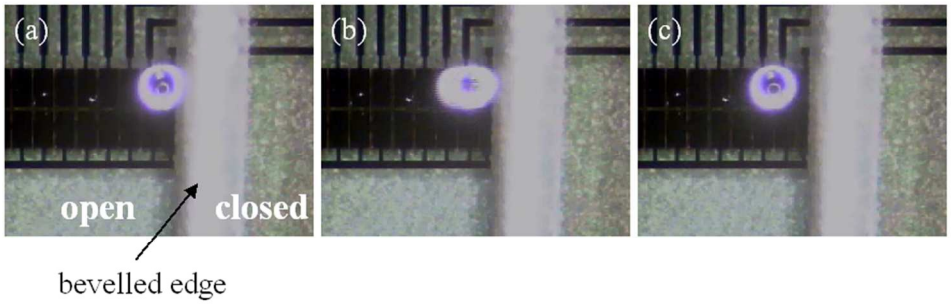

Fig. 9 Detachment of water drop from ITO plate with bevelled edge. AC applied voltage is 90 V_{rms} at 100 Hz. The beveled angle is around 40°. Video 02 can be seen in the ESI.

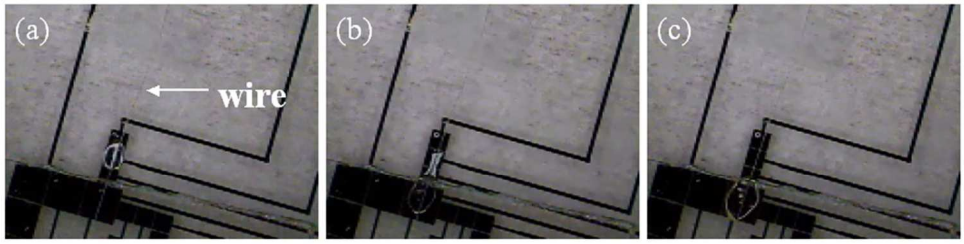

Fig. 10 Moving water drop across boundary from open to closed section. The voltage applied is 100 V_{rms} 100 Hz AC. Video 03 can be seen in the ESI.

Fig. 10 shows a sequence of video frames of the reverse process, that is, a water droplet driven from an open substrate into a closed section again via the electrowetting force. The electrode structure in this scheme is somewhat different: square electrodes at the bottom plate are individually addressable both in the open and closed sections, and a metal wire is used as the ground potential in the open section. The water droplet is successfully driven into the closed section at an actuation voltage of 100 V_{rms}. For this voltage, and without considering the saturation effect, the Lippmann-Young equation predicts a contact angle of $\theta_V = 61°$, which is at least consistent with the force analysis result presented earlier that θ_V must be less than 78°. Refer to Fig. 5a.

Comparison of behavior of water and oil droplets at open/ closed boundary

Fig. 11a shows selected video frames for a water droplet initially placed in a closed section (on the right) and a large silicone oil droplet in the adjacent open section (on the left). When the water droplet is ejected from the closed channel into the open section and makes contact with the oil droplet, the oil droplet tries to engulf the water drop and in so doing contacts the closed/open boundary. The oil droplet is then immediately drawn into the closed section by capillary forces. Contact with the water is retained but the oil drop resides in the closed section and the water droplet remains in the open section. This phenomenon has potential applications in separating oil/water mixtures.

Oil droplet movement between closed and open regions

The force balance analysis presented earlier predicts that movement of an oil droplet from a closed to an open section requires an oleophobic surface. We tested a Si wafer etched to form a two-dimensional array of reentrant pillars to achieve the required oleophobic behavior. This structured Si wafer was used as the top electrode in the closed section. Because Si is opaque, the droplet behavior was observed from the side. The fabrication process of oleophobic surface is similar to that of Tuteja et al.[40] and Wu et al.[41,42]. After fabrication, we measured the Cassie-Baxter state apparent contact angle for the three cap patterns, as shown in Table 2. In the experiments for electric field assisted microfluidic manipulation of oil droplets, we used re-entrant

Table 2. Contact angle values for sessile water and mineral oil droplets on re-entrant microstructures.

Lateral SiO_2 cap spacing (W) in μm	20		40		60	
Solid-liquid contact fraction (f_{SL})	0.33		0.22		0.17	
Equilibrium contact angle on smooth Si surface	water: 92°; mineral oil: 78°					
	water	mineral oil	water	mineral oil	water	mineral oil
contact angle calculated from Cassie- Baxter model	133°	127°	142°	137°	147°	143°
measured apparent contact angle on textured surface	142°	141°	145°	143°	146°	144°

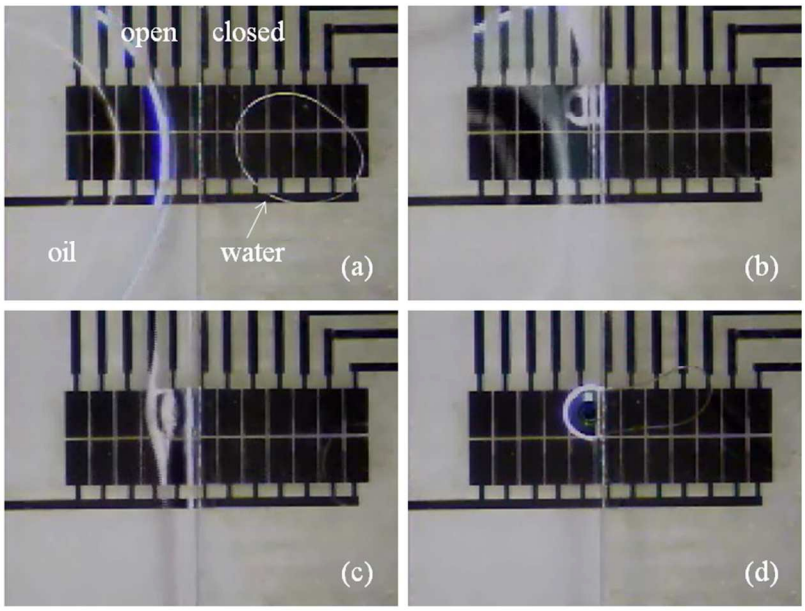

Fig. 11 Movement of oil droplet from open to closed section. (a) A water droplet placed in closed section (right) and a large silicone oil droplet placed in open section (left). (b) and (c) When the water droplet is delivered to open section, the oil droplet engulfs the water drop and moves into closed section. (d) Eventually, the oil droplet goes into closed section and the water drop stays in open section.

microstructures with 40 μm lateral spacing. The sequence of video frames in Fig. 12 shows the side view of a mineral oil droplet sandwiched in the 200 μm gap between a Teflon-coated glass substrate (below) and a textured Si substrate (above) being actuated by DEP. When the oil droplet reaches the boundary between the closed and open sections, it moves smoothly onto the open substrate.

Wu et al.[41] reported low resistance to motion when manipulating a hexadecane droplet in a parallel-plate structure with a textured Si wafer as the bottom substrate. In our experiment, the textured surface was on the top and we did not observe a significant change in the dynamic resistance since the actuation voltage was similar to that measured for the parallel glass plate device.

Double emulsion (DE) droplet formation and reseparation in an open region

We also investigated the behavior of water/oil double-emulsion droplets. Fig. 13 shows selected video frames of DE droplet formation. A water droplet is first dispensed from the left reservoir, and moved toward the closed/open boundary by EWOD actuation. When the droplet reaches the boundary, it is quickly ejected as shown in Figs. 13d and e. To detach this droplet, the ground ITO electrode on the upper substrate is disconnected and voltage is sequentially applied to the coplanar electrodes, as shown in Figs, 13f and g. The edge of the upper plate has been beveled to facilitate detachment. The water droplet is then transported towards a previously deposited oil droplet where, upon contact, the oil droplet spontaneously engulfs the water to form a DE droplet. The DE droplet can be transported by EWOD actuation as shown in Figure 13i. The gap spacing in the closed section is 90 μm, and the voltage applied through the entire process is 100 Vrms, 100 Hz AC.

If the DE droplet is now moved back to the boundary, upon reaching it the oil is drawn immediately into the closed section while the water droplet remains behind on the open substrate. The two droplets can now be separated using EWOD to detach the water droplet. As digital microfluidics handles not only water and oil droplets, but also molecules arranged along or transported across the water-oil interface, the separation of emulsion droplet could be useful in applications of sample extraction or concentration.

Discussion

The robustness of textured surfaces employed to achieve oleophobic behavior for oil droplet manipulation is a major concern. The apparent oleophobic behavior of an oil droplet is due to air pockets entrapped beneath the liquid. This condition is known as the Cassie-Baxter state[43]. If the air supporting the liquid is expelled, the liquid makes contact with the entire rough surface and the Cassie-Baxter state changes into the Wenzel state[44]. For oil droplets, the Cassie-Baxter state is in fact metastable because the intrinsic contact angle is less than 90°. A transition from the Cassie-Baxter to the Wenzel state occurs over time due to sagging of liquid-air interface. To investigate this transition, we

Table 3 Observed persistence time of apparent contact angles in the Cassie-Baxter state.

	Acetone	Corn oil	Sunflower oil	Castor oil	Mineral oil
Apparent contact angle (°)	132	130	124	146	143
Persistence time (min)	0.5±0.3	1.1±0.3	11.2±2.2	30.5±9.6	32.2±12.3

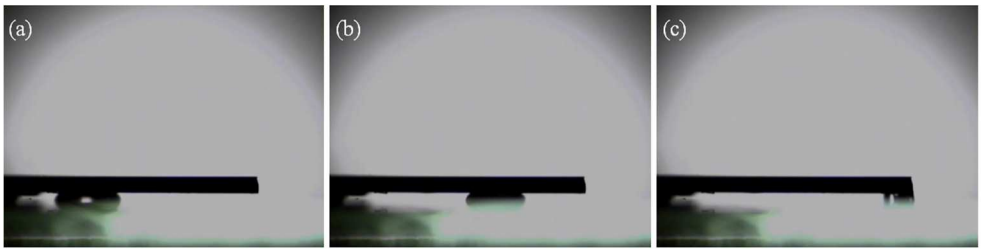

Fig. 12 Side view showing manipulation of mineral oil droplet between Teflon-AF treated glass substrate (bottom) and textured Si substrate (top). The spacing between two substrates is 200 μm. Applied AC voltage is 560 V_{rms} at 100 Hz. Video 04 can be seen in the ESI.

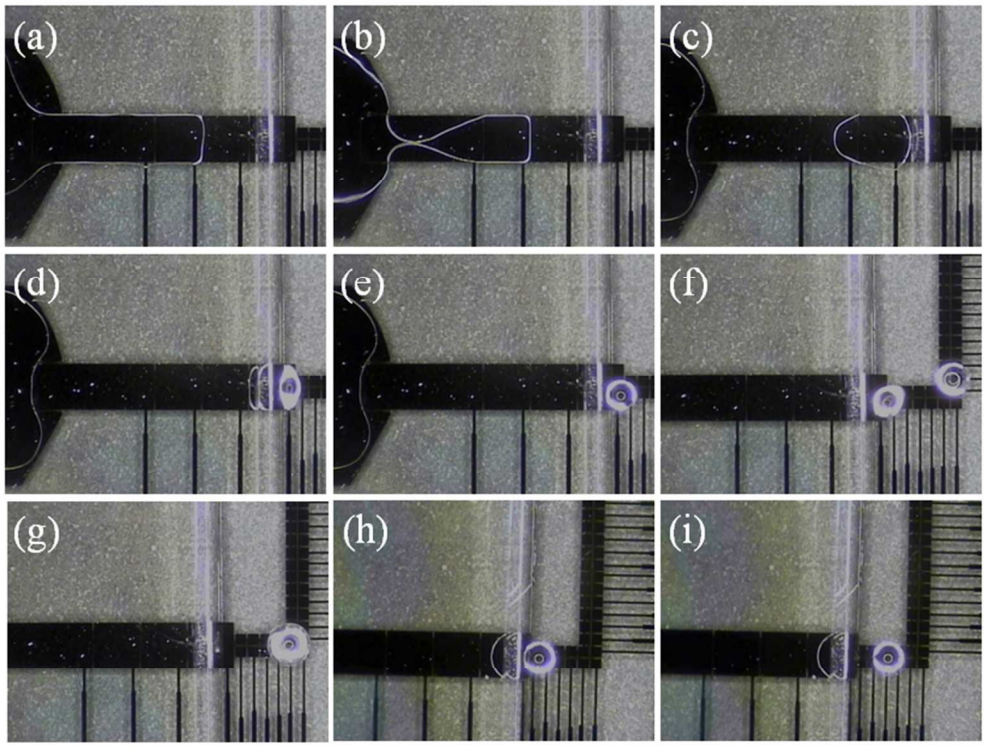

Fig. 13 Formation and separation of water-in-silicone oil DE droplet in open section. (a), (b) A water droplet is dispensed by EWOD actuation in closed section. (c) The water droplet is transported toward the closed/open boundary. (d), (e) The water droplet is ejected to the open section. (f) The water droplet is detached from the upper ITO substrate. (g) The water droplet is delivered and combined with a silicone oil droplet to form DE droplet. (h) The DE droplet is moved back to the closed/open boundary. When the DE droplet reaches the boundary, the oil droplet immediately goes into closed region. (i) The DE droplet is again separated into water (mostly) and oil droplets by detaching the water droplet. The voltage applied through the entire process is 100 Vrms, 100 Hz AC. Video 05 can be seen in the ESI.

measured the persistence time of apparent contact angles in the Cassie-Baxter state for several different oils by observations on static, sessile droplets. A 2 μL oil droplet was placed on the oleophobic surface, so that its initial apparent contact angle was > 90°. We then recorded the time for this oil droplet to drop below 90°. Each experiment was repeated three time and the results are tabulated in Table 3.

In addition to the problem posed by the Cassie-Baxter to Wenzel transition for static sessile droplets of oil, there is concern about their dynamic behavior when moving on substrates. A simple test shown in Fig. 14 was conceived to study the time course of the transition for droplets in motion. An mineral oil droplet was moved back and forth manually to observe the persistence of oleophobic behavior on a textured Si wafer. Typically, as shown in Fig. 14b, tiny oil droplets begin to detach and adhere to the textured surface after three cycles. This behavior indicates local transitions to the Wenzel state. After a few more cycles, more and more small droplets adhere to the surface. After about ten cycles, the entire oil drop pins and becomes unmovable.

Joly et al. used a finite element model to simulate the Cassie to Wenzel transition for a re-entrant pillar structure[45], finding that the liquid filling transition originates from a spontaneous filling of the cavities with liquid rather than a collapse of the meniscus. One hypothesis is that local condensation of the liquid at the internal corners of the cavity causes this transition. This explanation is consistent with the persistence time tests performed on sessile droplets, as seen in Table 3, the volatile acetone droplet stays in the Cassie-Baxter state for a very short time. If this transition mechanism is correct, an inverse-

trapezoidal re-entrant microstructure might be used to enhance the robustness of the Cassie-Baxter state[46]. Creating such a structure to achieve oleophobic behavior on a Si wafer is a serious fabrication challenge.

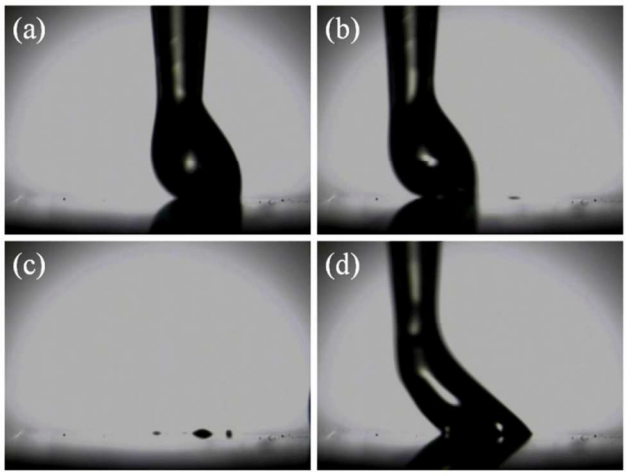

Fig. 14 Manual sliding of mineral oil droplet across textured oleophobic surface. (a) The first cycle. (b) After 3 cycles. (c) After 7 cycles. (d) The 10th cycle.

Conclusions

Microfluidic devices combining closed and open systems on a single substrate represent a potentially significant enhancement for droplet-based microfluidics in micro-total analysis systems. The ability to move liquid droplets freely back and forth between closed and open microfluidic systems would make it possible to exploit the advantages of both. In pursuit of this goal, we have investigated water and oil droplet movement across the boundary between closed and open microfluidic systems on a substrate.

Simple models based on Gibbs energy estimates and force balance exercises were presented to predict the requirements for moving liquid droplets across the boundary between closed and open microfluidic systems. The Gibbs free energy approach establishes certain ground rules for these droplet transitions, and the force balance analysis provides estimates for the voltage required to transfer a droplet between a closed and an open region in cases when the motion is opposed by capillarity. The model predicts that it is easy to move a water droplet from a closed to an open section, and that the reverse motion can be achieve using EWOD actuation. An oil droplet on the other hand, is energetically favored to stay in a closed section. Furthermore, driving an oil droplet from closed to open section by DEP actuation can be accomplished using an oleophobic treatment of the electrodes. The model allows a prediction of the voltage required to achieve this transition.

For experiments with water droplets, the voltage values required to achieve closed-to-open or open-to-closed movement agree reasonably well with modeling predictions. To encourage detachment of water droplets from the upper plate, beveling the edge of the upper electrode minimizes the water-Teflon contact thereby significantly reducing the required voltage. We also utilized an oleophobic surface treatment to demonstrate oil droplet movement from a closed to open structure. The oleophobic behavior is obtained with a re-entrant micropillar structure machined on a silicon wafer. Further effort in the fabrication of such surfaces will be needed to improve the robustness of such coatings.

Acknowledgments

The authors gratefully acknowledge David Harding, Paul Osborne, and Victor Derefinko at the University of Rochester, Greg Randall at General Atomics, and Michael Skvarla and Vince Genova at the Cornell NanoScale Science & Technology Facility (CNF) of Cornell University for their many insights and generous technical assistance. This work was supported by the US Department of Energy, Office of Inertial Confinement Fusion under Cooperative Agreement DE-FC52-08NA28302, the University of Rochester, and the New York State Energy Research and Development Authority.

References

1 R. B. Fair, *Microfluid. Nanofluid.*, 2007, **3**, 245-281.
2 F. Mugele, and J. C. Baret, *J. Phys.: Condens. Matter*, 2005, **17**, R705-R774.
3 A. R. Wheeler, *Science*, 2008, **322**, 539-540.
4 M. Abdelgawad, and A. R. Wheeler, *Adv. Mater.*, 2009, **21**, 920–925.
5 K. Choi, A. H.C. Ng, R. Fobel, and A. R. Wheeler, *Annu. Rev. Anal. Chem.,* 2012, **5**, 413-440.
6 S. K. Fan, T. H. Hsieh, and D. Y. Lin, *Lab chip*, 2009, **9**, 1236-1242.
7 W.-Q. Wang, T. B. Jones, and D. R. Harding, *Fusion. Sci. Tech*., 2011, **59**, 240-249.
8 J. A. Schwartz, J. V. Vykoukal, and P. R. C. Gascoyne, *Lab Chip*, 2004, **4**, 11-17.
9 O. D. Veleo, B. G. Prevo, and K. H. Bhatt, *Nature*, 2003, **426**, 515-516.
10 R. Ahmed, and T. B. Jones, *J. Electrost*., 2006, **64**, 543-549.
11 R. Ahmed, and T. B. Jones, *J. Micromech. Microeng*., 2007, **17**, 1052-1058.
12 W.-Q. Wang, and T. B. Jones, *J. Phys.: Conf. Ser*., 2011, **301**, 012057.
13 R. B. Fair, A. Khlystov, V. Srinivasan, V. K. Pamula, K. N. Weaver, *Proc of SPIE*, 2004, **5591**, 113-124.
14 C. G. Cooney, C. Y. Chen, M. R. Emerling, A. Nadim, J. D. Sterling, *Microfluid Nanofluid*, 2006, **2**, 435-446.
15 U. C. Yi, and C. J. Kim, *J. Micromech. Microeng*., 2006, **16**, 2053-2059.
16 M. Abdelgawad, and A. R. Wheeler, *Adv. Mater.,* 2007, **19**, 133-137.
17 P. Y. Paik, V. K. Pamula, K. Chakrabarty, *IEEE Tran Very Large Scale Integr (VLSI) Syst*., 2008, **16,** 432-443.
18 M. Abdelgawad, P. Park, and A. R. Wheeler, *J. Appl. Phys.*, 2009, **105**, 094506.
19 X.-Y. Zeng, K.-D. Zhang, J. Pan, G.-P. Chen, A.-Q. Liu, S.-K. Fan, and J. Zhou, *Lab Chip*, 2013, **13**, 2714-2720.
20 Y.-P. Zhao and Y. Wang, *Rev. Adhesion Adhesives*, 2013, **1**(1): 114-174.
21 P. Y. Keng, S. Chen, H. Ding, S. Sadeghi, G. J. Shah, et al. *Proc. Natl. Acad. Sci. USA*, 2012, **109**: 690–695.
22 H. C. Lin, Y. J. Liu, D. J. Yao, *J. Assoc. Lab. Autom.*, 2010, **15**: 210–215.
23 V. N. Luk, A. R. Wheeler, *Anal. Chem.*, 2009, **81**: 4524–4530.
24 M. J. Jebrail, H. Yang, J. M. Mudrik, N. M. Lafreniere, C. McRoberts, et al. *Lab Chip*, 2011, **11**: 3218–3224.
25 P. Dubois, G. Marchand, Y. Fouillet, J. Berthier, T. Douki, et al. *Anal. Chem.*, 2006, **78**: 4909–4917.
26 J. Gorbatsova, M. Jaanus, M. Kaljurand, *Anal. Chem.*, 2009, **81**: 8590–8595.
27 E. Berthier and D. J. Beebe, *Lab Chip*, 2007, **7**, 1475–1478.
28 M. Abdelgawad, M. W. L. Watson and A. R. Wheeler, *Lab Chip*, 2009, **9**: 1046–1051.

29 M. W. L. Watson, M. J. Jebrail, and A. R. Wheeler, *Anal. Chem.*, 2010, **82**: 6680–6686.

30 S. Schiaffino and A. A. Sonin, *J. Fluid Mech.*, 1997, **343**: 95-110.

31 J. Berthier, Microdrops and Digital Microfluidics, William Andrew, Norwich, NY, 2008.

32 W.-Q. Wang, On-Chip Double Emulsion Droplet Assembly Using Electrowetting-on-Dielectric and Dielectrophoresis, Ph.D. thesis, Chapter 1, University of Rochester, 2012.

33 J. Berthier, Ph. Clementz, J.M. Roux, Y. Fouillet, C. Peponnet, *Proc 2006 Nanotech Conf*, 2006, 685-688.

34 G. Wang, D. Teng, and S. K. Fan, *Proc. IEEE NEMS*, 2012, 415-418.

35 T. B. Jones, and K. L. Wang, *Langmuir*, 2004, **20**, 2813-2818.

36 T. B. Jones, *Langmuir,* 2002, **18**, 4437-4443.

37 F. Mugele, *Soft matter*, 2009, **5**, 3377-3384.

38 Q. Kang, D. Zhang, S. Chen, *Phys. Fluids*, 2002, **14**: 3203.

39 J. M. Roux, Y. Fouillet, and J. L. Achard, *Sens. Actuators A*, 2007, **134**: 486–493.

40 A. Tuteja, W. Choi, M. Ma, J. M. Mabry, S. A. Mazzella, G. C. Rutledge, G. H. McKinley, R. E. Cohen, *Science*, 2007, **318**: 1618-1622.

41 T. Wu, Y. Suzuki, *Lab Chip*, 2011, **11**: 3121-3129.

42 T. Wu, Y. Suzuki, *Sensor Actuator B*, 2011, **156**: 401-409.

43 A. B. D. Cassie, and S. Baxter, Wettability of porous surfaces, *Trans. Faraday Soc.*, 1944, **40**, 546-551.

44 R. N. Wenzel, Resistance of solid surfaces to wetting by water, *Ind. Eng. Chem.*, 1936, **28**, 988-994.

45 L. Joly, and T. Biben, *Soft Matter*, 2009, **5**, 2549-2557.

46 M. Im, H. Im, J.-H. Lee, J. B. Yoon, and Y. K. Choi, *Soft Matter*, 2010, **6**, 1401-1404.